

## Anodic oxidation of sulphite in alkaline aqueous solution on graphite electrode

A. Enache, M. Dan, A. Kellenberger, N. Vaszilcsin\*

University Politehnica Timisoara, Faculty of Industrial Chemistry and Environmental Engineering, Laboratory of Electrochemistry, Corrosion and Electrochemical Engineering, 6 Parvan, 300223 Timisoara, Romania

Received November 15, 2016      Revised December 28, 2016

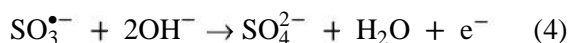
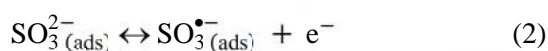
The anodic oxidation of sulphite in alkaline aqueous solution on graphite electrode has been studied by voltammetric methods and electrochemical impedance spectroscopy. The cyclic voltammograms allowed identification of the following processes that take place during anodic polarization of the working electrode: mediated oxidation of sulphite ions with adsorbed atomic oxygen, direct oxidation of sulphite on graphite and oxygen evolution. The kinetic parameters that characterize the charge transfer process have been determined by the Tafel method. The obtained Tafel slope ( $+0.123 \text{ V dec}^{-1}$ ) is close to the theoretical value ( $+0.118 \text{ V dec}^{-1}$ ) and therefore the charge transfer coefficient  $\tau$  tends to 0.5. A high value of the exchange current density  $i_0$  ( $1.9 \text{ A m}^{-2}$ ) has been obtained. Chronoamperometric and chronocoulometric measurements have been performed to evaluate the conversion degree of sulphite to sulphate. The results obtained by voltammetry experiments were confirmed by electrochemical impedance spectroscopy. The morphological changes of graphite electrode surface after a certain time of electrolysis have been highlighted by scanning electron microscopy.

**Key words:** anodic sulphite oxidation, graphite electrode, electrochemical impedance spectroscopy, chronoamperometry, chronocoulometry.

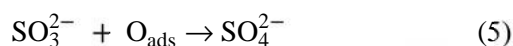
### INTRODUCTION

The favorable results of researches regarding the use of hydrogen sulfide in  $\text{H}_2\text{S}/\text{O}_2$  fuel cells [1,2] have focused the researchers interest on other sulfur compounds too. As a result, an opportunity to use sulfur compounds originating from recovery plants in refineries as fuel for alkaline fuel cells has been provided [3]. Generally, sulfur is recovered in refineries in the form of liquid volatile or gaseous compounds such as hydrogen sulfide, sulfur dioxide, carbonyl sulfide or carbon disulfide [4], what makes feasible their use in fuel cells. Large amounts of  $\text{SO}_2$  from combustion gasses of fossil fuels are recovered as sulphites. One way to exploit residual sulphites is given by their use in the alkaline  $\text{SO}_3^{2-}/\text{O}_2$  fuel cells. Since the composition of fuel cells electrodes is based on carbon materials with various graphitization degrees, it is necessary to carry out a systematic study of the electrochemical behavior of sulphites on graphite. The use of graphitic materials as electrodes for fuel cells has been widely studied due to the influence of their properties on the performance and lifetime of fuel cells [5-13]. Even in its manufacturing, the surface of graphite is modified with oxygenated functional groups, such as hydroxyl, carbonyl and/or carboxyl groups. Anodic polarization in aqueous solution

increases the number of these functional groups [14], but may also lead to degradation of graphite that occurs simultaneously with oxygen evolution reaction and forms either carbon dioxide in acid solutions, or carbonate ions in alkaline solutions [15]. Two mechanisms have been proposed for the alkaline oxidation of sulphites. In the systematic study of sulphite oxidation on graphite rotating disk electrode [16], direct oxidation mechanism carried out in 4 steps has been described as follows:



The second proposed mechanism of sulphite oxidation is described as a mediated oxidation with atomic oxygen adsorbed on the surface of graphite anode [17]:



It should be taken into account that in an aqueous sulphite solution, the chemical species  $\text{SO}_2$ ,  $\text{HSO}_3^-$  and  $\text{SO}_3^{2-}$  are present simultaneously in pH depending rates. In alkaline conditions at  $\text{pH} > 10$ , the sulphite ions are the predominant chemical species [18].

The aim of this work is to study electrochemical behavior of sulphite ions on graphite electrode, in order to identify the optimal conditions for recovering

To whom all correspondence should be sent:  
E-mail: nicolae.vaszilcsin@upt.ro

sulphites from the by-products of various technological processes. In addition, researches on electrochemical behavior of sulfur dioxide will allow its use in the  $\text{SO}_2/\text{O}_2$  fuel cell, which besides electricity will also produce sulfuric acid.

## EXPERIMENTAL

Electrolyte solutions were prepared using sodium hydroxide NaOH (Merck *p.a.*  $\geq 99\%$ ) and sodium sulphite  $\text{Na}_2\text{SO}_3$  (Merck *p.a.*  $\geq 98\%$ ).

Electrochemical studies were carried out using a Biologic SP 150 potentiostat/ galvanostat. The anodic oxidation of sulphite was studied by linear and cyclic voltammetry experiments and electrochemical impedance spectroscopy. The amount of oxidized sulphite as a function of potential was determined by chrono-methods (chronoamperometry and chronocoulometry).

All electrochemical experiments were performed in a glass electrolysis cell equipped with two graphite counter electrodes positioned symmetrically near the working electrode (graphite, geometric surface area of  $0.8 \text{ cm}^2$ ) and a silver-silver chloride Ag/AgCl reference electrode ( $E = +0.197 \text{ V/SHE}$ ). The surface of the working electrode was prepared by the mechanical polishing with SiC grinding paper #2400 and diamond paste  $3 \mu\text{m}$ , washed and ultrasonicated in distilled water for 10 minutes before each measurement. The anodic oxidation of sulphite was studied in  $1 \text{ mol.L}^{-1}$  NaOH solution as the supporting electrolyte with different concentrations of  $\text{Na}_2\text{SO}_3$ :  $10^{-3}$ ,  $10^{-2}$  and  $10^{-1} \text{ mol.L}^{-1}$ , at  $25^\circ\text{C}$ . All measurements were carried out in solutions purged with high purity nitrogen. Cyclic voltammograms were recorded at scan rates of 500 and  $100 \text{ mV s}^{-1}$  and linear polarization curves were obtained at the scan rate of  $1 \text{ mV s}^{-1}$ . Electrochemical impedance spectra were recorded in the frequency range 100 kHz to 10 mHz with alternating voltage signal amplitude of 10 mV. The surface morphology of graphite electrode before and after chronoamperometry measurements was studied by scanning electron microscopy (SEM) using a FEI INSPECT S microscope.

## RESULTS AND DISCUSSION

### Cyclic voltammetry

In order to identify the processes that take place at the electrode/electrolyte interface, cyclic voltammograms were recorded in  $1 \text{ mol L}^{-1}$  NaOH in the absence and presence of various concentrations of sodium sulphite:  $10^{-3}$ ,  $10^{-2}$  and  $10^{-1} \text{ mol.L}^{-1}$ , respectively. The first cycle voltammograms of the working electrode, recorded

after 5 minutes of conditioning at the open circuit potential are drawn in Fig. 1. Voltammograms presented in Fig. 1 indicate that at anodic polarization, the oxidation of sulphites occurs simultaneously with oxygen formation. These processes are accompanied by chemical transformation of the graphite surface, as it has been mentioned before.

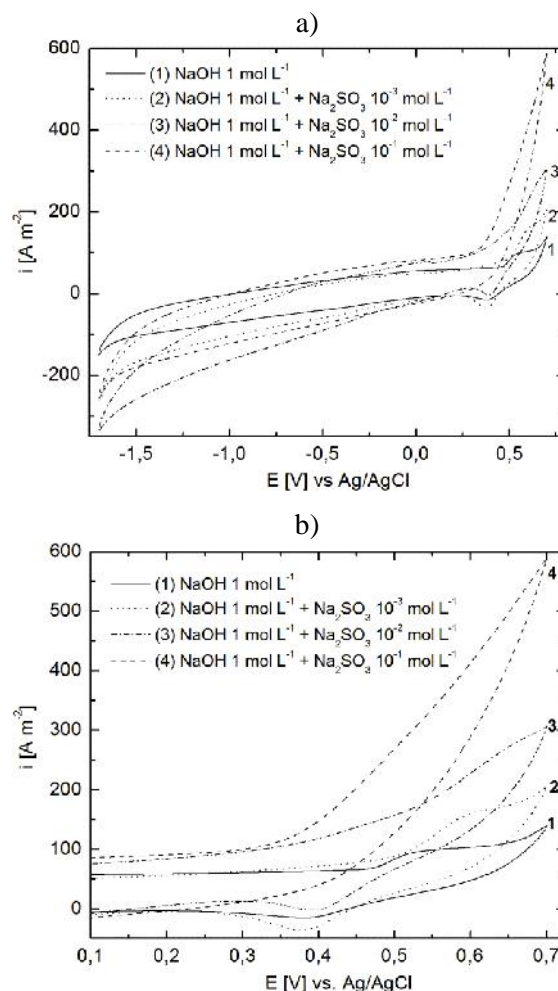
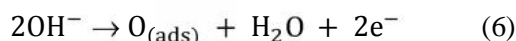


**Fig.1.** Cyclic voltammograms on graphite electrode in  $1 \text{ mol L}^{-1}$  NaOH solution with different concentrations of  $\text{Na}_2\text{SO}_3$  at  $500 \text{ mV s}^{-1}$ : a) voltammograms drawn over entire domain of the potential, b) zoom in the anodic area.

The cathodic peak observed at reverse potential sweep at about  $+0.38$  to  $+0.4 \text{ V}$  in both NaOH and NaOH+ $\text{Na}_2\text{SO}_3$  solutions is assigned to the reduction of oxygenated functional groups at the surface of graphite electrode [14], taking into account that it is not present on platinum [19]. Since in the presence of sulphite this peak does not significantly alter its shape and height, it can be concluded that oxidation of sulphite is an irreversible process. At advanced cathodic polarization, the hydrogen evolution takes place. Details of cyclic voltammogram (Fig. 1b, curve 1)

show that in the absence of sulphite ions, a limiting anodic current appears, which is attributed to formation of adsorbed atomic oxygen, according to the reaction (6) [20]:



By addition of small amounts of sulphite, the limiting current increases proportionally to its concentration (Fig. 1b, curves 2 and 3), what means that sulphite ions react with atomic oxygen adsorbed on the graphite surface. The continuous removal of adsorbed oxygen from the electrode surface enhances its formation reaction, and as a result the limiting current increases. Therefore, it can be concluded that at low concentrations, the anodic oxidation of sulphite ions in alkaline solution is mediated by the adsorbed oxygen, what is contrary to the results obtained by Lu *et al.* [16]. At higher concentrations of sulphite ( $\geq 10^{-1} \text{ mol L}^{-1}$ ), however, the anodic peak corresponding to the formation of adsorbed atomic oxygen is no longer observed. This is due to a facile access of sulphite ions to the electrode surface, where the oxygen mediated oxidation takes place concomitantly with direct oxidation of sulphite according to the mechanism proposed by Lu *et al.* [16]. At higher anodic potentials the oxygen evolution reaction takes place, as is highlighted on the cyclic voltammograms recorded in an extended potential range (Fig. 2).

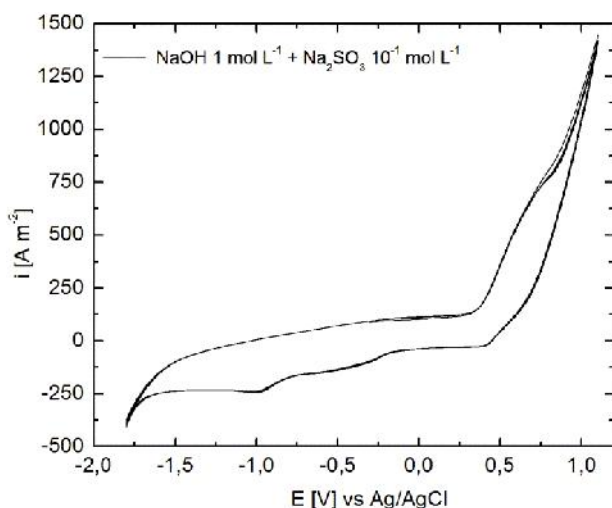


**Fig. 2.** Cyclic voltammograms (5 scans) on graphite electrode in  $1 \text{ mol L}^{-1}$  NaOH solution with  $10^{-1} \text{ mol L}^{-1}$   $\text{Na}_2\text{SO}_3$  at  $500 \text{ mV s}^{-1}$ .

To obtain information on the sulphite anodic oxidation in time, cyclic voltammograms were recorded with a large number of scans (25 scans) at a lower scan rate ( $100 \text{ mV s}^{-1}$ ). By analyzing cyclic voltammograms given in Fig. 3, one can observe significant reduction of limiting current density with increasing number of cycles.

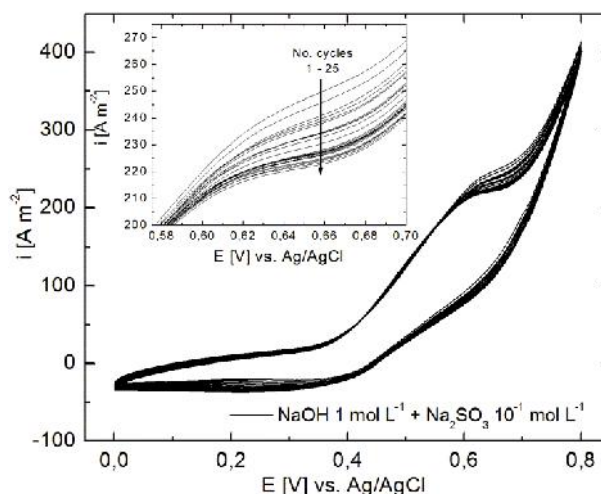


**Fig. 3.** Cyclic voltammograms – anodic branch (25 scans) on graphite electrode in  $1 \text{ mol L}^{-1}$  NaOH solution with  $10^{-1} \text{ mol L}^{-1}$   $\text{Na}_2\text{SO}_3$  at  $100 \text{ mV s}^{-1}$ . Inset: evolution of anodic limiting current density as function of number of cycles.

The inset in Fig. 3 shows decrease of the limiting current density by approximately 13% from about  $245 \text{ A m}^{-2}$  (scan 1) to  $215 \text{ A m}^{-2}$  (scan 25). This fact can be explained by continuous degradation of the graphite surface during cycling and by filling of graphite pores with oxygen leading to reduction of the active surface area of the electrode.

#### Linear voltammetry

Cyclic voltammograms obtained at high scan rates showed that at high sulphite concentrations ( $10^{-1} \text{ mol L}^{-1}$ ) the formation of adsorbed atomic oxygen takes place simultaneously with the direct oxidation of sulphite on the graphite electrode. Since the atomic oxygen formed on graphite is consumed entirely for the oxidation of sulphite, it can be considered that the total anodic current is used only for the oxidation of sulphite to sulphate. Therefore, the kinetic parameters that characterize the oxidation of sulphite, the anodic charge transfer coefficient  $\Gamma$  and exchange current density  $i_0$ , can be determined by the Tafel method for the potential range where the electrode process is controlled by charge transfer. It should, however, be noted that the values obtained in this case for  $\Gamma$  and  $i_0$  are just apparent values because they refer to an undefined process.

Since the kinetic parameters can be calculated for quasi-stationary conditions, linear polarization curves were obtained at low scan rates ( $1 \text{ mV s}^{-1}$ ) and presented in Fig. 4.

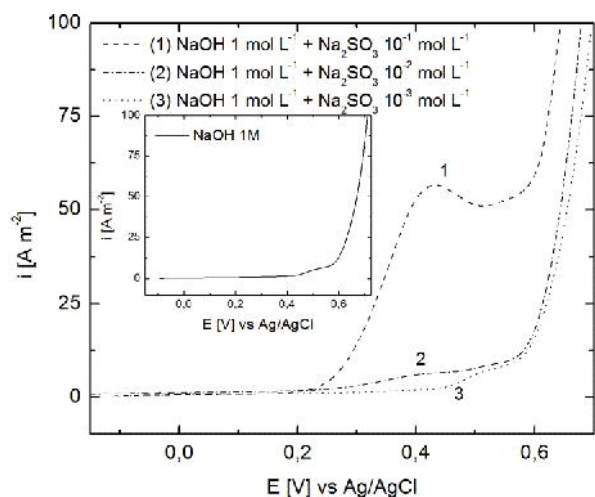


**Fig. 4.** Linear voltammograms on graphite electrode in alkaline solution with different concentrations of  $\text{Na}_2\text{SO}_3$  at  $1 \text{ mV s}^{-1}$ . Inset: linear voltammogram of the supporting electrolyte.

Each anodic overpotential ( $\eta$ ) value was calculated as the difference between the working electrode potential and the equilibrium potential. The equilibrium potential was approximated by extrapolating the linear part of the voltammogram (corresponding to charge transfer) to the abscissa. The dependence of  $\eta$  on the logarithm of current (Tafel plot) for the alkaline solution with  $10^{-1} \text{ mol L}^{-1} \text{ Na}_2\text{SO}_3$  is shown in Fig. 5, while the corresponding kinetic parameters are given in Table 1.

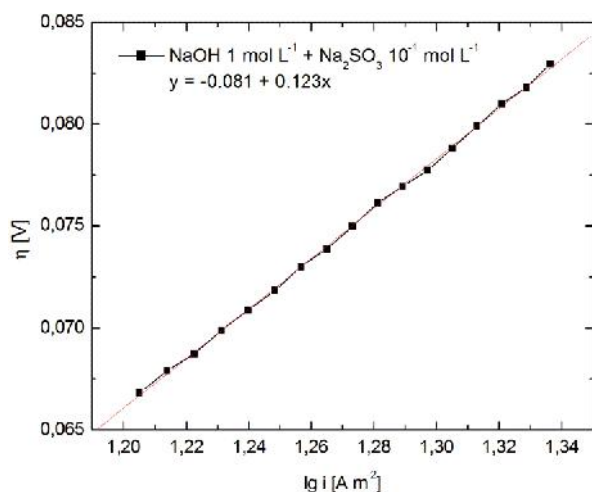


**Fig. 5.** Tafel plot for anodic oxidation of sulphite on graphite electrode in alkaline solution with  $10^{-1} \text{ mol L}^{-1} \text{ Na}_2\text{SO}_3$ .

The calculated value of the Tafel slope ( $+ 0.123 \text{ Vdec}^{-1}$ ) is close to the theoretical value of  $+ 0.118 \text{ Vdec}^{-1}$  for one-electron charge transfer process and the anodic charge transfer coefficient  $\Gamma$  is close to 0.5. A high value of the exchange current density is obtained ( $1.9 \text{ A m}^{-2}$ ), what is characteristic for the fast charge transfer processes and comparable to that obtained by other authors on skeletal nickel [17]. In these circumstances, it can be evaluated

that the rate determining step for formation of atomic oxygen is the charge transfer process that leads to formation of  $\text{HO}\ddot{\text{O}}$  radicals adsorbed on the graphite according to the following reaction [19]:



Similarly, for the direct oxidation of sulphite, the rate determining step is the charge transfer given by equation (2).

**Table 1.** Kinetic parameters for  $10^{-1} \text{ mol L}^{-1}$  sulphite in alkaline solution.

$\text{Na}_2\text{SO}_3$ concentration [ $\text{mol L}^{-1}$ ]	$b$ [ $\text{mV dec}^{-1}$ ]	$\Gamma$	$i_0$ [ $\text{A m}^{-2}$ ]
$10^{-1}$	123	0.48	1.9

#### Chronoamperometry and chronocoulometry

For establishing potential step values applied in the chronoamperometric and chronocoulometric study of the anodic oxidation of sulphite, the linear voltammogram obtained on graphite in  $10^{-1} \text{ mol L}^{-1} \text{ Na}_2\text{SO}_3$  was used. Six potential steps were chosen (0.25, 0.35, 0.45, 0.55, 0.65 and 0.75 V) to highlight the anodic processes that take place. The applied DC potential was maintained for one hour and the corresponding current – time curves were recorded, as shown in Fig. 6.

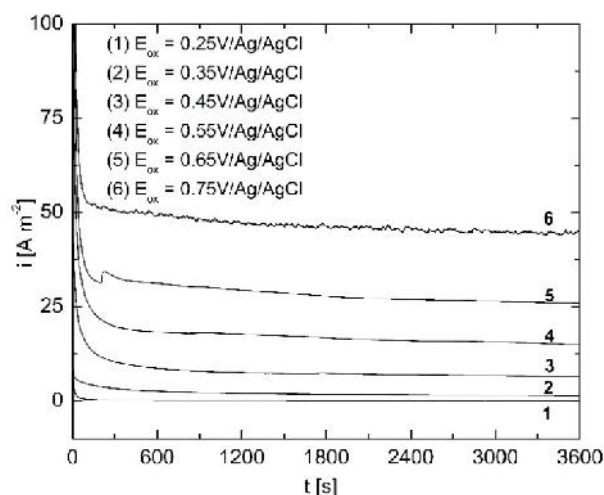


**Fig. 6.** Current-time curves on graphite in  $1 \text{ mol L}^{-1} \text{ NaOH} + 10^{-1} \text{ mol L}^{-1} \text{ Na}_2\text{SO}_3$  solution.

Each of the chronoamperometric curves obtained for the first 5 potential steps is characterized by a decay of the current followed by a plateau of constant and smooth currents, suggesting that the anodic processes (mediated oxidation and direct oxidation of sulphite) are taking place without major variation of the resistance of the solution, *i.e.* without oxygen release. Curve 6, obtained for the applied potential

of +0.75 V shows obvious irregularities, indicating that in parallel to oxidation of sulphite to sulphate, the reaction of oxygen evolution occurs. The significant increase of current density at the electrode potential of +0.75 V is another evidence of the oxygen evolution reaction. Therefore, only for the first five electrode potential step values, one can admit that the entire amount of electricity through the electrode is used exclusively for the oxidation of sulphite to sulphate, *i.e.* the current efficiency for the oxidation of sulphite to sulphate is 100%.

Similar chronoamperometric curves were also obtained for sulphite concentrations of  $10^{-2}$  and  $10^{-3}$  mol L<sup>-1</sup>, indicating that the potential for the oxygen evolution reaction shifts to more negative values as the concentration of sulphite decreases. Thus, for  $10^{-3}$  mol L<sup>-1</sup> sulphite solution, the oxygen release starts at the electrode potential of +0.65 V. It was also noted that the values of quasi-stationary current densities are increased after 1 hour as has been expected for the increasing concentration of sulphite.

Chronoamperometric curves obtained for three different concentrations of sulphite at electrode potentials where oxygen evolution does not take place were integrated to obtain the amount of electricity passing at the anode. Based on the

Faraday's laws, the amount of sulphite oxidized to sulphate (  $\delta$  ) has been calculated, together with the degree of transformation (  $r$  ) of sulphite to sulphate. These two parameters are represented as a function of the electrolysis time in Fig. 7, showing the chronocoulometric curves for the base solution with  $10^{-1}$  mol L<sup>-1</sup> Na<sub>2</sub>SO<sub>3</sub>. Table 2 gives the chronoamperometric and chronocoulometric data for all three concentrations of sulphite.

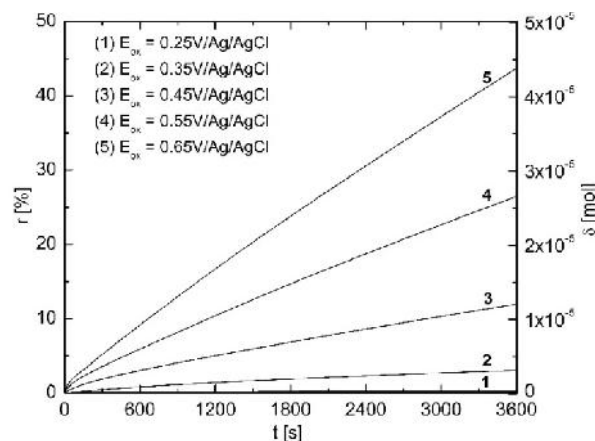


Fig. 7. Chronocoulometric curves on graphite in 1 mol L<sup>-1</sup> NaOH + 10<sup>-1</sup> mol L<sup>-1</sup> Na<sub>2</sub>SO<sub>3</sub> solution.

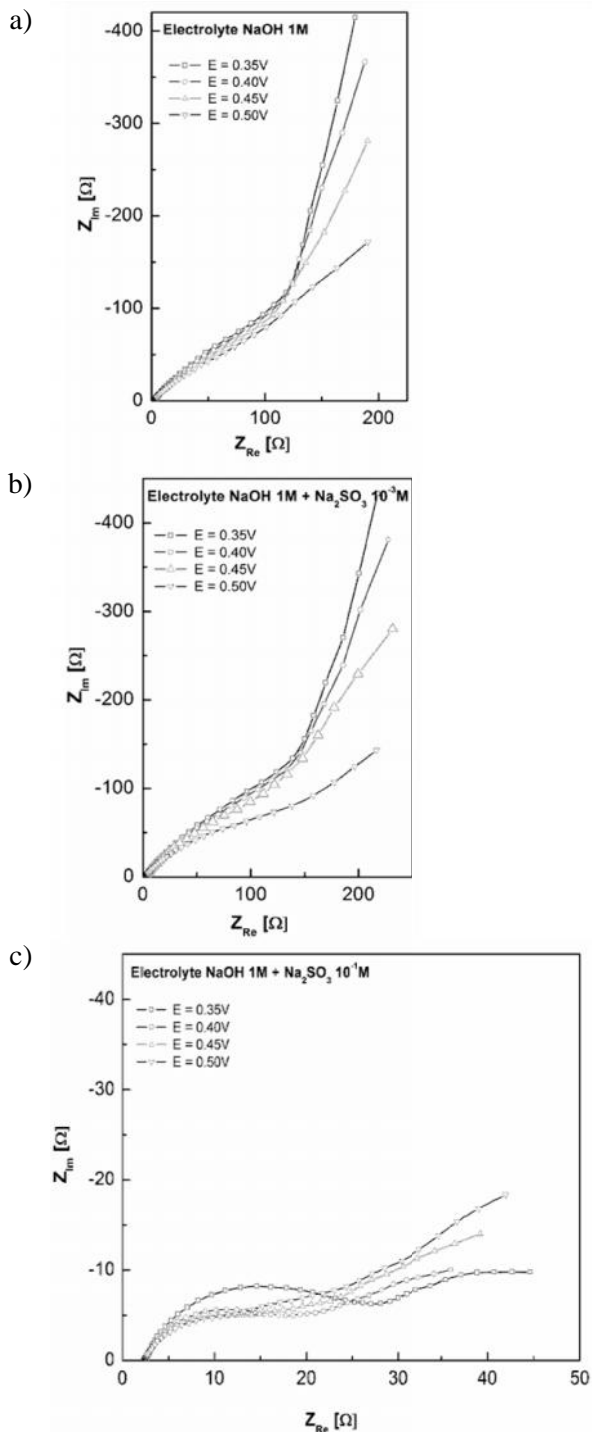
The linear dependence of  $r$  and  $\delta$  over time is another argument indicating that current efficiency for the oxidation of sulphite to sulphate is 100%.

Table 2. Chronoamperometric and chronocoulometric measurements on graphite electrode in 1 molL<sup>-1</sup> NaOH solution with different concentrations of Na<sub>2</sub>SO<sub>3</sub>.

Na <sub>2</sub> SO <sub>3</sub> concentration [mol L <sup>-1</sup> ]	E [V] vs. Ag/AgCl	Chronoamperometric measurements				Chronocoulometric measurements			
		$i_{\text{final}}$ [A m <sup>-2</sup> ]				$r$ [%]			
		$t$ [min]				$t$ [min]			
10 <sup>-3</sup>	0.25	0.11	0.07	0.06	0.05	0.15	0.19	0.21	0.23
	0.35	0.17	0.13	0.12	0.11	0.13	0.18	0.23	0.27
	0.45	0.42	0.33	0.28	0.26	0.27	0.40	0.52	0.62
	0.55	2.79	2.46	2.29	2.18	1.52	2.50	3.39	4.22
	0.65	43.09	41.26	40.00	39.04	-	-	-	-
10 <sup>-2</sup>	0.25	0.20	0.16	0.14	0.13	0.20	0.30	0.33	0.38
	0.35	0.69	0.61	0.52	0.56	0.40	0.60	0.87	1.07
	0.45	1.20	1.06	1.01	0.94	0.70	1.14	1.52	1.89
	0.55	3.43	3.15	2.95	2.91	1.93	3.16	4.43	5.40
	0.65	47.57	44.00	41.85	40.23	-	-	-	-
10 <sup>-1</sup>	0.25	1.20	1.10	1.06	1.01	0.63	0.92	1.03	1.49
	0.35	2.28	1.81	1.59	1.48	1.23	1.98	2.61	3.17
	0.45	7.91	7.36	6.84	6.52	4.16	6.84	9.58	12.06
	0.55	18.03	16.74	15.75	14.87	8.26	14.80	20.81	26.55
	0.65	30.32	27.76	26.64	25.85	13.07	23.91	34.01	43.80
	0.75	48.28	46.60	45.43	44.96	-	-	-	-

*Electrochemical impedance spectroscopy*

Electrochemical impedance spectra were recorded at several electrode potentials in the range +0.35 to +0.50 V, for the base solution in the absence and in the presence of various concentrations of sulphite ions. Typical Nyquist plots are given in Fig. 8.



**Fig. 8.** Nyquist plots for sulphite oxidation on graphite in 1 mol L<sup>-1</sup> NaOH solution: (a) without sulphite, (b) with 10<sup>-3</sup> mol L<sup>-1</sup> Na<sub>2</sub>SO<sub>3</sub> and (c) with 10<sup>-1</sup> mol L<sup>-1</sup> Na<sub>2</sub>SO<sub>3</sub>.

In the absence and at low concentrations of sulphite, the shape of the complex plane plots is characterized by the presence of a high frequency semicircle for the charge transfer process followed by diffusion at low frequencies, corresponding to the formation of adsorbed atomic oxygen. In the presence of low concentrations of sulphite (10<sup>-3</sup> mol L<sup>-1</sup>) the diameter of the charge transfer semicircle starts to decrease at higher potentials due to the onset of sulphite oxidation process. At high concentration of sulphite (10<sup>-1</sup> mol L<sup>-1</sup>) the high frequency semicircle is well pronounced and its radius is potential dependent, so it can be attributed to the charge transfer of direct oxidation process. The oxidation of sulphite starts at lower electrode potentials. The Randles equivalent circuit was fitted to measured impedance spectra and the impedance of the faradic reaction was expressed by charge transfer resistance  $R_{ct}$  and Warburg diffusion element. The results of the complex non-linear fittings are given in Table 3.

*Scanning electron microscopy*

The morphology of the graphite electrode surface was studied by scanning electron microscopy. Fig. 9 shows the SEM images of the working electrode before and after chronoamperometric measurements of sulphite oxidation carried out in alkaline solution.

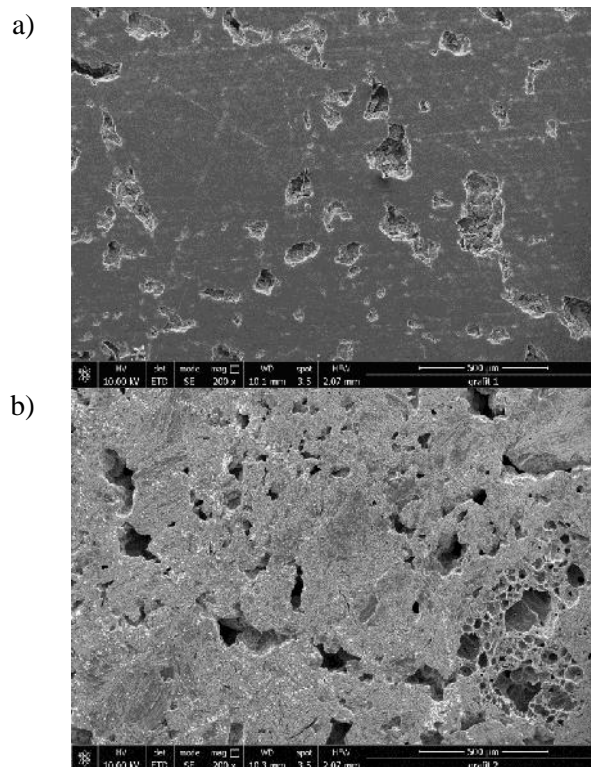


**Fig. 9.** SEM images before (a) and after (b) chronoamperometric studies, magnification 200.

**Table 3.** Fitting results and standard errors for equivalent circuit parameters related to oxidation of sulphite on graphite in 1 mol L<sup>-1</sup> NaOH in the presence of 10<sup>-1</sup> mol L<sup>-1</sup> Na<sub>2</sub>SO<sub>3</sub>.

	$E = 0.35 \text{ V}$	$E = 0.40 \text{ V}$	$E = 0.45 \text{ V}$	$E = 0.50 \text{ V}$
$R_s$ [ $\text{cm}^2$ ]	2.4 (0.2%)	2.4 (0.2%)	2.4 (0.2%)	2.4 (0.2%)
$T$ [F $\text{cm}^{-2} \text{ s}^{n-1}$ ]	0.00305 (1.4%)	0.00311 (2.0%)	0.00350 (3.0%)	0.00384 (3.7%)
$n$	0.78 (0.3%)	0.78 (0.4%)	0.77 (0.6%)	0.75 (0.8%)
$C_{dl}$ [F $\text{cm}^{-2}$ ]	$9.13 \times 10^{-4}$	$8.56 \times 10^{-4}$	$8.26 \times 10^{-4}$	$7.81 \times 10^{-4}$
$R_{ct}$ [ $\text{cm}^2$ ]	20.6 (1.4%)	12.6 (2.1%)	10.0 (3.2%)	8.7 (4.2%)
$R_d$ [ $\text{cm}^2$ ]	34.4 (3.3%)	43.0 (4.4%)	69.8 (7.4%)	118.5 (30.1%)
$\tau_d$ [s]	41.1 (9.6%)	107.7 (15.5%)	246.6 (25.1%)	703.8 (> 30%)
$p$	0.36 (2.2%)	0.32 (2.0%)	0.31 (1.8%)	0.32 (1.6%)

By analyzing the SEM images in Fig. 9, it can be emphasized that the initial surface of the graphite electrode is smooth, showing only slight defects originated from the finishing process. The SEM images after the chronoamperometry experiments show that the electrooxidation of sulphite influences the morphology of the electrode, most likely because in alkaline medium at high anodic potentials, the formation of carbonate ions occurs. Even if the rate of carbonate ions formation is reduced, the effect on the morphology of graphite electrode is significant. In time, the increase of the specific surface is favorable for the oxidation of sulphite to sulphate, but after longer electrolysis time the graphite electrode should be replaced.

## CONCLUSIONS

Cyclic voltammetry studies revealed that at low current densities and low concentrations of sulphite in alkaline solution, the oxidation of sulphite is mediated by atomic oxygen adsorbed on the graphite electrode surface. At high concentrations of sulphite (>10<sup>-1</sup> mol L<sup>-1</sup>), due to a good access of sulphite ions to the electrode surface, the direct oxidation of sulphite takes place together with mediated oxidation. At significantly high current densities, the oxygen evolution reaction occurs in parallel with both above mentioned oxidation processes.

The Tafel method was used to determine the kinetic parameters characterizing the anodic process in the range of charge transfer control. The obtained slope (+0.123 V dec<sup>-1</sup>) is indicative for one-electron transfer process. Consequently, the resulting value of the anodic charge transfer coefficient is close to 0.5. It is noteworthy that the exchange current density has a quite high value, specific for fast electron transfer reactions.

Chronoamperometry curves confirmed that at advanced anodic polarization the oxidation of sulphite to sulphate is accompanied by oxygen evolution reaction. By integrating chronoamperometric curves at potentials where there is no oxygen release, chronocoulometric curves were obtained. Since the chronocoulometric curves, showing the dependence of the amount of transformed sulphite and the degree of transformation of sulphite to sulphate as a function of electrolysis time, are quasi-linear dependencies, it can be stated that the current efficiency for sulphite oxidation is close to 1. As a result, the formation rate of oxygenated functional groups on the graphite surface and of carbon dioxide evolution is reduced.

Different shapes of the electrochemical impedance spectra were obtained for the oxidation of low and high concentrations of sulphite, in accordance with the two different oxidation routes proposed, mediated oxidation and direct oxidation of sulphite.

**Acknowledgements:** This work was partially supported by the University Politehnica Timisoara within the frame of PhD studies.

## REFERENCES

- 1.D. Uzun, E. Razkazova-Velkova, V. Beschkov, *J. Appl. Electrochem.*, **46**, 943 (2016).
- 2.N. Dermendzhieva, E. Razkazova-Velkova, V. Beschkov, *Bulg. Chem. Comm.*, **49**, 793 (2015).
- 3.V. Beschkov, private communication.
- 4.T. Whaley, G. Long, Sulfur and Hydrogen Sulfide Recovery, in *Petroleum Technology*, Wiley Critical Content, 2007, p. 872.
- 5.T.M. Gur, R.A. Huggins, *J. Electrochem. Soc.*, **139**, L95 (1992).
- 6.M. Ihara, K. Matsuda, H. Sato, C. Yokoyama, *Solid State Ion.*, **175**, 51 (2004).

7. X. Cheng, L. Chen, C. Peng, Z. Chen, Y. Zhang, Q. Fanc, *J. Electrochem. Soc.*, **151**, 48 (2004).
8. J. Wang, G. Yin, Y. Shao, S. Zhang, Z. Wang, Y. Gao, *J. Power Sources*, **171**, 331 (2007).
9. C.H. Paik, G.S. Saloka, G.W. Graham, *Electrochem. Solid-State Lett.*, **10**, 39 (2007).
10. K.H. Lim, H-S. Oh, S-E. Jang, Y.-J. Ko, H-J. Kim, H. Kim, *J. Power Sources*, **193**, 575 (2009).
11. C.A. Reiser, L. Bregoli, T. W. Patterson, J. S. Yi, J. D. Yang, M.L. Perry, T. D. Jarvi, *Electrochem. Solid-State Lett.*, **8**, 273 (2005).
12. H.-S. Oh, J.-H. Lee, H. Kim, *Int. J. Hydrogen Energy*, **37**, 10844 (2012).
13. S. Maass, F. Finsterwalder, G. Frank, R. Hartmann, C. Merten, *J. Power Sources*, **176**, 444 (2008).
14. I. Radoi, C. Daminescu, G. Musca, Z. Popa, *Revista de Chimie*, **40**, 202 (1989).
15. A. L. Dicks, *J. Power Sources*, **156**, 128 (2006).
16. J. Lu, D. Dreisinger, W. Cooper, *J. App. Electrochem.* **29**, 1161 (1999).
17. A. Enache, N. Vaszilcsin, M. Dan, *Chem. Bull. Politehnica Univ. (Timisoara)* **61**, 12 (2016).
18. J. O'Brien, J. Hinkley, S. Donne, S-E. Lindquist, *Electrochim. Acta*, **55**, 573 (2010).
19. E. Skavas, T. Hemmingsen, *Int. J. Electrochem. Sci.* **2**, 203 (2007).
20. D. Santos, C.A.C. Sequeira, *Quim. Nova*, **36**, 1176 (2013).

\*

6, 300,223

15 2016 .; 28 2016 .  
( )

(+0.123 V dec-1)

(0.118 V dec-1),

io (1.9 Am-2).

0,5.